VARIATION OF THE ^{111}CD - P POPULATION IN SILICON WITH ANNEALING TEMPERATURE.

By

Temesgen Yirdaw

A THESIS PRESENTED TO

THE SCHOOL OF GRADUATE STUDIES

ADDIS ABABA UNIVERSITY

IN PARTIAL FULFILLMENT OF THE REQUIREMENTS

FOR THE DEGREE OF

MASTER OF SCIENCE in PHYSICS

ADDIS ABABA, ETHIOPIA

AUGUST 2007

ADDIS ABABA UNIVERSITY

DEAPRMENT OF PHYSICS

The undersigned hereby certify that they have read and recommend to the Faculty of Science for acceptance of an MSc Thesis entitled "**Variation Of the ^{111}Cd - P population in Silicon with Annealing Temperature.**" by **Temesgen Yirdaw** in partial fulfillment of the requirements for the degree of **Master of Science**.

Dated: August 2007

Supervisor: _____
Dr. Genene Tessema

Examiners: _____
Pro. Singh K.P.

_____
Dr. Tilahun T.

This Work is Dedicated to My Family

Table of Contents

List of Tables

List of Figures

Acknowledgements

I have a very high gratitude to my advisor, Dr. Genene Tessema for his excellent guidance, wise advise and strong motivation through out the process of this study. I am also quite grateful to my parents for their financial and moral support.

Many thanks goes to my friends Buzea G|micheal and Melaku Tesfay for their constructive discussions that I have had with them that put significant input for the successful completion of this study I wish to express my gratitude to the Department of Physics, Addis Ababa University.

At last but certainly not the least I want to thank my **God** for giving me the strength and courage to complete this task by setting every thing ready for me.

Addis Ababa University Temesgen Yirdaw

July, 2007

Abstract

Studying the nature of defects in semiconductor helps to minimize the undesired behaviors they contribute. In this study, the perturbed angular correlation method has used to understand the formation of the substitutional $^{111}Cd-P$ pairs in silicon. The pairs are characterized by a unique quadrupole interaction frequency of $\nu_Q = 179$MHz, that suggest a strong interaction between acceptor and donor atoms in an elemental semiconductor silicon. The variation of the nearest neighbor $^{111}Cd - P$ population with the annealing temperature is discussed. Finally, the binding energy and ratios of free and trapped states around the complex are determined using the fraction of the probe atom that form the pairs at annealing temperature intervals of $700^oC - 1000^oC$.

Chapter 1

Introduction

Semiconductor has contributed tremendously to the progress in the areas of communication, information technology, solar energy conversion and many other fields [7]. The most commonly used elemental semiconductor materials are silicon and germanium. Another interesting class of materials can be created by introducing impurities in a controlled manner into the lattice of a semiconductor. The major effects of an impurity in a regular semiconductor crystal lattice is that it introduces a low density of allowable energy levels into the normally forbidden region[10]. The presence of such energy levels can alter the properties of the materials, that may happen intentionally or undesirable during the material processes. Investigation of the impurity properties are important on controlling the properties of the host material. The impurities may create defects, which can change the properties of the material, such as: the electrical as well as the optical properties of the host material [12].

Generally, defects in solids such as, intermetallic compounds, metal oxides, semiconductor and insulators, induce characteristic electric field gradient (EFG) at atomic lattice sites. The EFG can be observed via the interaction of the field with the nuclear electric quadrupole moment of a suitable probe atom. This type of interaction is called Hyperfine interaction. Studies of hyperfine interactions may be carried out by several methods using stable or unstable nuclei. High resolution optical spectroscopy and nuclear magnetic resonance (NMR) utilize the ground state

of stable nuclei where as Mössbauer spectroscopy and perturbed angular correlations (PAC) uses excited states of unstable nuclei. All the techniques have proven in the past to be versatile tools for studying a broad range of problems of nature [9].

The perturbed angular correlation technique is being used to measure the hyperfine interaction, that exist due to the presence of defects in semiconductors and other materials. This nuclear technique relies on unstable radioactive probe atom like ^{111}In. The quantity measured is the electric field gradient (EFG), which arises from the charges of the immediate lattice surrounding at the site of the probe atom. The probe atom (^{111}In) is used to extract information about the microscopic environments of the probe. Information about the nature of defects trapped at the probe site can be obtained through this interaction.

The formation of pairs and complexes between the ionized impurities or defects in group IV semiconductors has been studied extensively by the perturbed $\gamma - \gamma$ angular correlation spectroscopy. Besides, the interest in this work is to study the properties of impurity pairs between a substitutional acceptor and other impurity atom from group V donors in Si. Through PAC analysis, correlating changes in microscopic configuration of the indium ions with macroscopic factors like temperature can yield useful information about the behavior of defect-impurity complexes.

The theoretical background of the method used is discussed in chapter two and three of this thesis. The experimental results of the indium phosphorous pairs in silicon is presented in chapter 4. In the same chapter the population variation of the In-P pair with annealing temperature and the binding energy of the complex are discussed.

Chapter 2

HYPERFINE INTERACTION

2.1 Introduction

The microscopic environment of a solid is investigated by nuclear techniques whose working principles are based on the interaction between the nuclear moments (electric or magnetic) of the probe nucleus and the surrounding electromagnetic fields. The fields are usually caused by the charges from atoms in the vicinity of the nucleus or by the external sources. The interaction of moments of the nucleus with electromagnetic fields is called Hyperfine Interaction. This interaction induce changes in the nuclear and atomic energy level [7, 11].

2.2 Classical Electrostatic Hyperfine interaction

Classically, in solid the electrostatic energy of the nuclear charge, described by $\rho(r)$ under the influence of the potential $\phi(\overrightarrow{r})$, which is created by the charges from the atom in the vicinity of the nucleus [11], is given by:

$$E_{inte} = \int \rho(\overrightarrow{r})\phi(\overrightarrow{r})dr^3 \tag{2.1}$$

Where $\int \rho(\overrightarrow{r})dr^3 = ze$ is the total nuclear charge. Assuming that $\phi(\overrightarrow{r})$ changes slowly in the region where $\rho(r)$ is non vanishing it may be expanded in a Taylor

series in the vicinity of $r = 0$:

$$\phi(r) = \phi(0) + \sum_{\alpha=1}^{3} \left(\frac{\partial \phi}{\partial x_\alpha}\right)_0 + \frac{1}{2} \sum_{\alpha,\beta=1}^{3} \left(\frac{\partial^2 \phi}{\partial x_\alpha x_\beta}\right)_0 x_\alpha x_\beta + ... \tag{2.2}$$

Inserting equation (2.2) and the expression for the nuclear charge into (2.1), then electrostatic energy has a form

$$\begin{aligned} E_{int} &= \phi(0)ze + \sum_{\alpha=1}^{3} \left(\frac{\partial \phi}{\partial x_\alpha}\right)_0 \int \rho(r) x_\alpha d^3 r \\ &+ \frac{1}{2} \sum_{\alpha,\beta=1}^{3} \left(\frac{\partial^2 \phi}{\partial x_\alpha \partial x_\beta}\right)_0 \int \rho(r) x_\alpha x_\beta d^3 r + .. \end{aligned} \tag{2.3}$$

Then a monopole, a dipole and quadrupole interaction energy results; where the monopole term will induce no degeneracy splitting and it is the coulomb energy of point charges. The coulomb energy contribute only to the potential energy of the crystal lattice. The second term corresponds to the dipole interaction which vanishes for nuclear states with a well defined parity since the dipole moment of a nucleus is zero. The third term includes the isomeric shift and the quadrupole interaction. The expansion shows the characteristic way in which the various multipoles interact with an external field, such as the charge with the potential, the dipole with the electric field, the quadrupole with the field gradient. So, the first and second terms will not have any relevance on this discussion. The interaction energy is left only with the quadrupole interaction energy, that is

$$E_{int} = \frac{1}{2} \sum_{\alpha,\beta=1}^{3} \left(\frac{\partial^2 \phi}{\partial x_\alpha \partial x_\beta}\right)_0 \int \rho(r) x_\alpha x_\beta d^3 r \tag{2.4}$$

By adding and subtracting the monopole like term, which is

$$\frac{1}{6} \sum_{\alpha,\beta=1}^{3} \left(\frac{\partial^2 \phi}{\partial x_\alpha \partial x_\beta}\right)_0 \int \rho(r) r^2 d^3 r$$

with $r^2 = \sum_\alpha x_\alpha^2$ into equation (2.4) and the result would be.

$$\begin{aligned} E_{int} &= \frac{1}{6}\sum_{\alpha,\beta=1}^{3}\left(\frac{\partial^2\phi}{\partial x_\alpha x_\beta}\right)_0 \int \rho(r) r^2 d^3r \\ &+ \frac{1}{6}\sum_{\alpha,\beta=1}^{3}\left(\frac{\partial^2\phi}{\partial x_\alpha \partial x_\beta}\right)_0 \int \rho(r)(3x_\alpha x_\beta - r^2\delta_{\alpha\beta}) d^3r \end{aligned} \tag{2.5}$$

Where the second derivatives of the quantity $\phi_{\alpha\beta} = \partial^2\phi/\partial x_\alpha \partial x_\beta$ form a symmetric (3×3) matrix which can be diagonalized by a convenient rotation of the coordinate system. The electrostatic potential $\phi(\overrightarrow{r})$ obeys the Poisson equation $\Delta\phi = -4\pi\rho_e(r)$, where $\rho_e(r)$ is the electronic charge density, in holding particularly for $r = 0$ we get:

$$(\Delta\phi)_0 = \left(\sum_{\alpha=0}^{3}\phi_{\alpha\alpha}\right)_0 = 4\pi e|\psi(0)|^2 \tag{2.6}$$

where $-e\left|\psi\left(0\right)\right|^2$ is the charge density of the atomic electrons at the nucleus. The electrostatic hyperfine interaction is therefore:

$$\begin{aligned} E_{int} &= \frac{2\pi e}{3}|\psi\left(0\right)|^2 \int \rho\left(r\right) r^2 d^3r \\ &+ \frac{1}{6}\sum_{\alpha,\beta=1}^{3}\left(\frac{\partial^2\phi}{\partial x_\alpha \partial x_\beta}\right)_0 \int \rho\left(r\right)\left(3x_\alpha x_\beta - r^2\delta_{\alpha\beta}\right) d^3r \end{aligned} \tag{2.7}$$

$$E_{int} = E_M + E_Q$$

The isomeric shift E_M reflects the interaction between the extended charges of the nucleus and the electronic density at the nucleus. The quadrupole term E_Q gives the interaction between the electric field gradient tensor and the quadrupole moment tensor which describes the non spherical nuclear charge distribution.

2.2.1 The Monopole term Interaction (E_M)

From equation (2.7) the monopole term depends only on the mean square of the nuclear radius. This term gives a shift but no splitting of the levels and it describes the electrostatic interaction of an extended nucleus with the electrons at the nuclear site, that is the situation where electrons are present at the origin and these electrons determine the external potential field, which subsequently becomes spherically symmetric.

$$E_M = \frac{2\pi e}{3}|\psi(0)|^2 \int \rho_n(r) r^2 d^3r \tag{2.8}$$

2.2.2 The Electrostatic Quadrupole Interaction (E_Q)

In situation where a vanishing electron density at the origin occurs $\Delta\phi = 0$, in this case the particular term can be written as.

$$E_Q = \frac{1}{6}\sum_{\alpha,\beta=1}^{3}\left(\frac{\partial^2\phi}{\partial x_\alpha \partial x_\beta}\right)_0 \int \rho(r)(3x_\alpha x_\beta - r^2\delta_{\alpha\beta})d^3r \tag{2.9}$$

This is the quadrupole interaction energy. If the nuclear charge is distributed according to a smooth function, $\rho(\overrightarrow{r})$, then an analysis in multipole moments can be made. These moments are quite important in determining the potential in some point p at large distance compared to the nuclear charge extension. The potential can be calculated as

$$\phi(\overrightarrow{R}) = \frac{1}{4\pi\epsilon_0}\int_{vol}\frac{\rho(\overrightarrow{r})dr}{|\overrightarrow{R} - \overrightarrow{r}|} \tag{2.10}$$

For small values of $|r/R|$, we can express $1/|R - r|$ using the binomial expansion.

$$\frac{1}{|\overrightarrow{R} - \overrightarrow{r}|} = \frac{1}{(R^2 + r^2 - 2\overrightarrow{R}\cdot\overrightarrow{r})^{\frac{1}{2}}} = \frac{1}{R(1 + \frac{r^2}{R^2} - \frac{2\overrightarrow{R}\cdot\overrightarrow{r}}{R^2})^{\frac{1}{2}}} \tag{2.11}$$

$$\frac{1}{|\overrightarrow{R} - \overrightarrow{r}|} = \frac{1}{R}[1 + \frac{\overrightarrow{r}\cdot\overrightarrow{R}}{R^2} - \frac{r^2}{2R^2} + \frac{3}{2}(\frac{\overrightarrow{r}\cdot\overrightarrow{R}}{R^2})^2 - \frac{3}{8}(\frac{r^2}{R^2})^2 + \frac{6(\overrightarrow{r}\cdot\overrightarrow{R})^2}{2r^4} - ...]$$

$$\frac{1}{|\overrightarrow{R}-\overrightarrow{r'}|} \approx \frac{1}{R}\frac{\overrightarrow{R}\cdot\overrightarrow{r'}}{R^2} + \frac{3}{2}(\frac{\overrightarrow{R}\cdot\overrightarrow{r'}}{R^2})^2 - \frac{r^2}{R^2}]$$

$$= \frac{1}{R} + \frac{\overrightarrow{R}\cdot\overrightarrow{r'}}{R^3} + \frac{1}{2}[\frac{3(\overrightarrow{R}\cdot\overrightarrow{r'})^2}{R^5} - \frac{r^2}{R^3}] \tag{2.12}$$

When we expand the above terms, we can ignore these terms having the term r^4/R^4. Substitute the expressions in equation (2.12) in to equation (2.10), then

$$\begin{aligned}\phi(R) &= \frac{1}{4\pi\epsilon_0}\int_{vol}\frac{\rho(r)d\overrightarrow{r'}}{|\overrightarrow{R}|} + \frac{1}{4\pi\epsilon_0}\int_{vol}\frac{\rho(r)\overrightarrow{R}\cdot\overrightarrow{r'}d\overrightarrow{r'}}{|\overrightarrow{R}|^3} \\ &- \frac{1}{8\pi\epsilon_0}\int_{vol}\frac{\rho(r)r^2d\overrightarrow{r'}}{|\overrightarrow{R}|^3} + \frac{3}{4\pi\epsilon_0}\int_{vol}\frac{\rho(r)(\overrightarrow{R}\cdot\overrightarrow{r'}d\overrightarrow{r'})^2}{|\overrightarrow{R}|^5}d^3r\end{aligned}$$

$$\phi(\overrightarrow{R}) = \frac{q}{4\pi\epsilon_0 R} + \frac{1}{4\pi\epsilon_0}\int\frac{\rho(\overrightarrow{r'})r\cos\theta}{R^2}d^3r + \frac{1}{8\pi\epsilon_0}\int\frac{\rho(\overrightarrow{r'})(3\cos^2\theta-1)r^2}{r^3}d^3r \tag{2.13}$$

From the definition dot product, $\overrightarrow{R}\cdot\overrightarrow{r'} = Rr\cos\theta$ and this can be expressed using tensor form as $r\cos\theta = \frac{\overrightarrow{R}\cdot\overrightarrow{r'}}{R} = \sum_{i,j=1}^{3}\frac{X_i x_j}{R}$ and $(\overrightarrow{R}\cdot\overrightarrow{r'})(\overrightarrow{R}\cdot\overrightarrow{r'}) = \sum_{i,j=1}^{3}X_i x_j x_i X_j$ with the coordinate corresponding to x,y,z respectively for $i,j = 1,2,3$ using the cartesian coordinates we obtain

$$\phi(R) = \frac{1}{4\pi\epsilon_0}\frac{q}{r} + \sum_i\frac{P_i X_i}{4\pi\epsilon_0 R^3} + \sum_{ij}\frac{Q_{ij}}{8\pi\epsilon_0}X_i X_j \tag{2.14}$$

with

$$P_i = \int\rho(\overrightarrow{r'})x_i d^3r$$

$$Q_{i,j} = \int\rho(\overrightarrow{r'})(3x_i x_j - r'^2\delta_{ij})d^3r \tag{2.15}$$

The dipole components and quadrupole tensor, respectively .The quadrupole tensor Q_{ij} can be expressed via its nine components in matrix form as follows

$$Q_{ij} \Rightarrow \begin{pmatrix} 3x^2-r'^2 & 3xy & 3xz \\ 3yx & 3y^2-r'^2 & 3yz \\ 3zx & 3zy & 3z^2-r'^2 \end{pmatrix} \tag{2.16}$$

By choosing appropriate coordinate system the Q_{ij} can be transformed into diagonalized matrix in which the non-diagonal terms vanish and one gets new quadrupole tensor

$$Q_{ij} \Rightarrow \begin{pmatrix} 3x'^2-r'^2 & 0 & 0 \\ 0 & 3y'^2-r'^2 & 0 \\ 0 & 0 & 3z'^2-r'^2 \end{pmatrix} \tag{2.17}$$

The quantity $Q_{z'z'} = \int \rho(\overrightarrow{r'})(3z'z' - r'^2 d^3r$ denoted as the quadrupole moment of the charge distribution, relative to the axis system (x',y',z')

2.3 Quantum mechanical treatment of the electrostatic hyperfine interaction

The interaction between quadrupole moment of the nucleus and the local electric field gradient results in a splitting of the energy levels of the different states of the nucleus. The nuclear eigenstates may be characterized by the angular momentum quantum numbers I and m. In this representation the energy of the electrostatic interaction is given by the matrix element of the Hamiltonian [3,5]:

$$E_m = \langle Im|H_{el}|Im'\rangle \tag{2.18}$$

with

$$H_{el} = \sum_{c,p} \frac{e_p e_c}{|r_p - r_c|} \tag{2.19}$$

the sum is extended to all the nuclear and extra nuclear charges p and c respectively. Where e_p is the point charges in the nucleus at the points (r_p, θ_p, ϕ_p) and e_c are point charges (ions in the crystal lattice) at a position (r_c, θ_c, ϕ_c). For $r_c > r_p$, the term $\frac{1}{|r_p - r_c|}$ of the above expression can be written as the expansion of Legender polynomials [22].

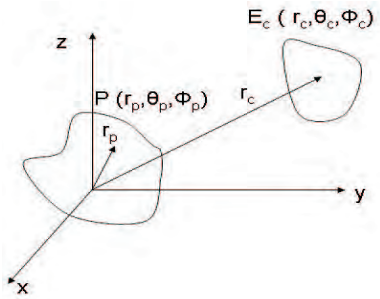

Figure 2.1: Nuclear and Extra nuclear charge distribution

$$\frac{1}{|r_p - r_c|} = \sum_{k=0}^{\infty} \frac{r_p^k}{r_c^{k+1}} p_k(\cos(r_p, r_c)) \tag{2.20}$$

Where p_k is the legender polynomial. Now we use the addition theorem of spherical harmonics, which states that; Two vectors r_p and r_c, with spherical coordinates (θ_1, ϕ_1) and (θ_2, ϕ_2) respectively are separated by an angle θ [4] and is defined

$$p_k(\cos\theta) = \frac{4\Pi}{2k+1} \sum_{k=-q}^{k} Y_k^q(\theta_1, \phi_1) Y_k^{-q}(\theta_2, \phi_2) \tag{2.21}$$

Hence, we can write equation (2.21) by replacing $Y_k^{-q} = (-1)^q Y_k^{q^*}$. Where Y_k^q is a spherical harmonic; which is defined by [22]

$$Y_k^q(\theta, \phi) = \frac{(-1)^q}{2^k k} \sqrt{\frac{(2k+1)}{4\pi}} \frac{(k-q)}{(k+q)} e^{iq\phi} (1 - \cos^2\theta)^{\frac{q}{2}} \frac{d^{k+q}}{d\cos\theta^{k+q}} (\cos^2\theta - 1)^k \tag{2.22}$$

This is the explicit form for $q > 0$. For negative q values, one has the relation above and when $q = 0$ equation (2.22) becomes

$$Y_k^0(\theta, \phi) = \sqrt{\frac{(2k+1)}{4\pi}} \frac{d^k(\cos^2\theta - 1)^k}{2^k k!(d\cos\theta)^k} \tag{2.23}$$

Therefore, substituting equation (2.21) and equation (2.22) into equation (2.20) and then substituting the result into equation (2.19) one obtains

$$H_{el} = 4\Pi \sum_{k=0}^{\infty} \frac{1}{2k+1} \sum_q (-1)^q \sum_p e_p r_p^k Y_{k,q}(\theta_p, \phi_p) \sum_c \frac{e_c}{r_c^{k+1}} Y_{k,-q}(\theta_c, \phi_c) \tag{2.24}$$

This may be written in a more compact way by introducing the tensor operators for the nuclear moments $T_q^{(k)}$ and the external field $V_q^{(k)}$ (k is the rank of the tensor):

$$T_q^k = \sum_p e_p r_p^k Y_{k,q}(\theta_p, \phi_p)$$

$$V_q^k = \sum_c \frac{e_c}{r_c^{k+1}} Y_{k,-q}(\theta_c, \phi_c) \tag{2.25}$$

From the definition of scalar product of two tensors of the same rank is given by [5]

$$T^k V^k = \sum_{q=-k}^{k} (-1)^q T_q^k V_q^k \tag{2.26}$$

the Hamiltonian may be written

$$\begin{aligned} H_{el} &= \sum_{k=0}^{\infty} \frac{4\pi}{2k+1} T^k V^k = 4\pi \frac{Ze}{4\pi} V(0) + \frac{1}{3} \sum (-1)^q T_q^1 V_q^1 + \\ &\times \frac{1}{5} \sum (-1)^q T_q^2 V_q^2 + \frac{1}{7} \sum (-1)^q T_q^3 V_q^3 + ...] \end{aligned} \tag{2.27}$$

The first term is the Coulomb term. The expectation values of T^1 (electric dipole moment) and of T^3 (electric octuple moment) are zero, since the nucleus is symmetric. Higher order moments are usually very small and can be neglected. We are therefore left with the Hamiltonian operator for the electric quadrupole interaction:

$$T^2 V^2 = \frac{4\pi}{5} \sum_q (-1)^q T_q^2 V_q^2 \tag{2.28}$$

The electric field gradient tensor V^2 can be expressed in an arbitrary cartesian coordinate system (x, y, z) using coulomb's law. Taking into account its symmetry

$$V_c = \sum_c \frac{e_c}{r_c} = \sum_c \frac{e_c}{\left[x^2 + y^2 + z^2\right]^{\frac{1}{2}}} \tag{2.29}$$

When we differentiate V_c with respect to z twice and express the result in polar coordinate by substituting $r \cos\theta$ in place of z, one gets

$$\frac{\partial^2 V_c}{\partial z^2} = \frac{1}{r^3} \sum_c e_c (3\cos^2\theta - 1) \tag{2.30}$$

Similarly, differentiate with respect to x and y respectively. The results are

$$\frac{\partial^2 V_c}{\partial x^2} = \frac{1}{r^3} \sum_c e_c (3\sin^2\theta \cos^2\phi - 1) \tag{2.31}$$

$$\frac{\partial^2 V_c}{\partial y^2} = \frac{1}{r^3}\sum_c e_c(3\sin^2\theta\sin^2\phi - 1) \tag{2.32}$$

The results for the mixed derivatives are also obtaining

$$\frac{\partial^2 V_c}{\partial x \partial y} = \frac{1}{r^5}\sum_c e_c xy = \frac{1}{r^3}\sum_c e_c \sin^2\theta\cos\phi\sin\phi \tag{2.33}$$

$$\frac{\partial^2 V_c}{\partial x \partial z} = \frac{1}{r^5}\sum_c e_c xz = \frac{1}{r^3}\sum_c e_c \sin\theta\cos\phi\cos\theta \tag{2.34}$$

$$\frac{\partial^2 V_c}{\partial y \partial z} = \frac{1}{r^5}\sum_c e_c yz = \frac{1}{r^3}\sum_c e_c \sin\theta\sin\phi\cos\theta \tag{2.35}$$

By symmetry

$$\begin{aligned} \frac{\partial^2 V_c}{\partial x \partial y} &= \frac{\partial^2 V_c}{\partial y \partial x} \\ \frac{\partial^2 V_c}{\partial x \partial z} &= \frac{\partial^2 V_c}{\partial z \partial x} \\ \frac{\partial^2 V_c}{\partial y \partial z} &= \frac{\partial^2 V_c}{\partial z \partial y} \end{aligned} \tag{2.36}$$

Generally, one can express equations using matrix

$$\frac{\partial^2 V}{\partial x_\alpha \partial x_\beta} = \sum_c \frac{e_c}{r^3}\begin{pmatrix} 3\sin^2\theta\cos^2\phi - 1 & \sin^2\theta\cos\phi\sin\phi & \sin\theta\cos\phi\cos\theta \\ \sin^2\theta\cos\phi\sin\phi & 3\sin^2\theta\sin^2\phi - 1 & \sin\theta\sin\phi\cos\theta \\ \sin\theta\cos\phi\cos\theta & \sin\theta\sin\phi\cos\theta & 3\cos^2\theta - 1 \end{pmatrix} \tag{2.37}$$

The electric field gradient tensor V_q^2 can be expressed in cartesian coordinate system (x,y,z). Taking into account its symmetry and Laplace equation $\triangle V = 0$ (considering only the charge distribution which is external to the nucleus) only five independent components remain expressed. From the general definition of the field tensor, i.e. from equation (2.25)

$$V_q^2 = \sum_c \frac{e_c}{r_c^{k+1}} Y_{k,-q}(\theta_c, \phi_c) \tag{2.38}$$

$$V_0^2 = \sqrt{\frac{5}{16\pi}}\frac{1}{r^3}\sum_c e_c(3\cos^2\theta - 1) \tag{2.39}$$

Since from equation (2.30) $V_{zz} = \frac{1}{r^3}\sum_c e_c(3\cos^2\theta - 1)$ and substitute this into equation (2.39) one can get

$$V_0^2 = \sqrt{\frac{5}{16\pi}}V_{zz} \tag{2.40}$$

Where $V_{zz} = \frac{\partial^2 V_c}{\partial z^2}$

$$V_{\pm 2}^2 = \frac{1}{r^3}\sum_c e_c\sqrt{\frac{15}{32\pi}}\sin^2\theta e^{\pm i2\phi} \tag{2.41}$$

Here we have used $Y_{2,\pm 2} = \sqrt{\frac{15}{32\pi}}\sin^2\theta e^{\pm i2\phi}$. Taking the real part only

$$V_{\pm 2}^2 = \frac{1}{r^3}\sum_c e_c\sqrt{\frac{15}{32\pi}}\sin^2\theta(\cos^2\phi - \sin^2\phi) \tag{2.42}$$

By subtracting equation (2.31) from (2.32), one can get

$$\frac{V_{xx} - V_{yy}}{3} = \frac{1}{r^3}\sum_c e_c\sin^2\theta(\cos^2\phi - \sin^2\phi) \tag{2.43}$$

Therefore, $V_{\pm 2}^2 = \sqrt{\frac{15}{32\pi}}\frac{V_{xx}-V_{yy}}{3} = \frac{1}{4}\sqrt{\frac{5}{6\pi}}\eta V_{zz}$. Where $\eta = \frac{V_{xx}-V_{yy}}{V_{zz}}$

$$V_{\pm 1}^2 = \sum_c \frac{e_c}{r^3}Y_{2,\pm 1}$$

$$V_{\pm 1}^2 = \sum_c \frac{e_c}{r^3}\sqrt{\frac{15}{8\pi}}e^{\pm i\phi}\sin\theta\cos\theta \tag{2.44}$$

Where, $Y_{2,\pm 1} = \sqrt{\frac{15}{8\pi}}e^{\pm i\phi}\sin\theta\cos\theta$. If we consider only the real part

$$V_{\pm 1}^2 = \sum_c \frac{e_c}{r^3}\sqrt{\frac{15}{8\pi}}\sin\theta\cos\theta\cos\phi \tag{2.45}$$

Generally, the electrostatic gradient tensor V can always be referred to a coordinate system xyz (principle axis system) such that the off-diagonal elements vanish.

Then, the number of components may be further reduced by a suitable transformation to the principal axis.

$$V_0^2 = \frac{1}{4}\sqrt{\frac{5}{\pi}}V_{zz}$$
$$V_{\pm 1}^2 = 0 \tag{2.46}$$
$$V_{\pm 2}^2 = \frac{1}{4}\sqrt{\frac{5}{6\pi}}\eta V_{zz}$$

The electric field gradient is characterized by the parameters V_{zz} and η. With the convention $|V_{xx}| \leq |V_{yy}| \leq |V_{zz}|$ the asymmetry parameter η has values in the range $0 \leq \eta \leq 1$. When the field gradient has axial symmetry, as for hexagonal or tetragonal lattices, the components V_{xx} and V_{yy} are equal and the electric field gradient is given by

$$V_0^2 = \frac{1}{4}\sqrt{\frac{5}{\pi}}V_{zz} \tag{2.47}$$

Substitute equation (2.47) into equation (2.28), then the Hamiltonian H_Q can be written as

$$H_Q = \sqrt{\frac{\pi}{5}}T_0^2 V_{zz} \tag{2.48}$$

With the quadrupole interaction energy given by:

$$E_m = \langle Im|H_Q|Im\rangle = \sqrt{\frac{\pi}{5}}V_{zz}\langle Im|T_0^2|Im\rangle \tag{2.49}$$

The quadrupole moment of the nucleus is defined as the maximum Z component (I=m) of the quadrupolar tensor as [1, 18]:

$$eQ = \langle II|\sum_p \rho_p(3z_p^2 - r_p^2)|II\rangle = \langle II|\sum_p \rho_p r_p^2(3\cos^2\theta - 1)|II\rangle \tag{2.50}$$

But, the second rank tensor operator of the nuclear quadrupole moment was defined in equation (2.26), using this equation, one can get

$$T_0^2 = \sum_p \frac{\rho_p r_p^2}{4}\sqrt{\frac{5}{\pi}}(3\cos^2\theta - 1)$$

Where $Y_{2,0} = \sqrt{\frac{5}{16\pi}}(3\cos^2\theta - 1)$

$$\frac{T_0^2}{\sqrt{\frac{5}{16\pi}}} = \sum_p \rho_p r_p^2 (3\cos^2\theta - 1) \tag{2.51}$$

Using equation (2.51) into equation (2.50), then

$$eQ = \langle II | \frac{T_0^2}{\sqrt{\frac{5}{16\pi}}} | II \rangle$$

$$eQ = 4\sqrt{\frac{\pi}{5}} \langle II | T_0^2 | II \rangle \tag{2.52}$$

This equation is solved Using the Wigner-Eckart theorem and the $3-j$ symbols (in Appendix $A.1$ and $A.2$)[10, 15] and then equation (2.49) become:

$$E_m = (-1)^{I-m} \sqrt{\frac{\Pi}{5}} V_{zz} \begin{pmatrix} I & 2 & I \\ -m & 0 & m \end{pmatrix} \langle I \| T^2 \| I \rangle \tag{2.53}$$

$$eQ = 4\sqrt{\frac{\Pi}{5}} \begin{pmatrix} I & 2 & I \\ -I & 0 & I \end{pmatrix} \langle I \| T^2 \| I \rangle$$

$$\langle I \| T^2 \| I \rangle = \frac{eQ}{4\sqrt{\frac{\Pi}{5}} \begin{pmatrix} I & 2 & I \\ -I & 0 & I \end{pmatrix}} \tag{2.54}$$

Inserting (2.54) into (2.53) and evaluating the $3-j$ symbols leads to the energy eigenvalues of the quadrupole interaction

$$E_m = \frac{3m^2 - I(I-1)}{4I(2I-1)} eQV_{zz} \tag{2.55}$$

Due to the m^2-dependence of the quadrupole interaction energy, there is still a two fold degeneracy of each energy levels. The energy difference between the two

consecutive sub states m and m' is then given by

$$E_m - E_{m'} = \frac{3eQV_{zz}}{4I(2I-1)} \left| m^2 - m'^2 \right| \tag{2.56}$$

The fundamental frequency of the interaction (ω_Q) [15]is now defined as

$$\omega_Q = \frac{3eQV_{zz}}{4I(2I-1)\hbar} \tag{2.57}$$

$$E_m - E_{m'} = 3\omega_Q \hbar \left| m^2 - m'^2 \right| \tag{2.58}$$

$$\omega_0 = \begin{cases} 6\omega_Q & \text{for half integral}, \\ 3\omega_Q & \text{for integral}. \end{cases}$$

where ω_0 is the frequency which corresponds to the smallest non-vanishing energy difference.

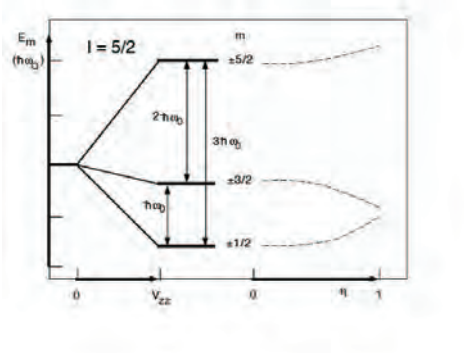

Figure 2.2: The splitting of the intermediate energy level for the spin $I = 5/2$.

When the field gradient is not axial symmetric $(\eta \neq 0)$ the influence of η on the energies of the m states may be easily understood if we write the quadrupole interaction with Hamiltonian as a function of the angular momentum operators as [1,3,11]:

$$H_Q = 3I_z^2 - I(I+1) + \frac{\eta}{2}\{I_+^2 + I_-^2\}\hbar\omega_Q \tag{2.59}$$

where I_z, I_+ and I_- are designate angular momentum operators. The quantities ω_Q and η are defined in Equation (2.58) and equation (2.44) respectively. In order to calculate the energy eigenvalues, the interaction matrix $\langle Im|H_Q|Im'\rangle$ has to be diagonalized. This can be achieved by the unitary transformation of the Hamiltonian (H_Q). For the spin $I = \frac{5}{2}$ the resulting energy eigenvalues are [5,7]

$$\begin{aligned} E_{\pm\frac{5}{2}} &= E_0 + 2\alpha\hbar\omega_Q(\frac{1}{3}arc\cos\beta) \\ E_{\pm\frac{3}{2}} &= E_0 - 2\alpha\hbar\omega_Q(\frac{1}{3}(\pi + arc\cos\beta)) \\ E_{\pm\frac{1}{2}} &= E_0 - 2\alpha\hbar\omega_Q(\frac{1}{3}(\pi - arc\cos\beta)) \end{aligned} \tag{2.60}$$

Where α and β are

$$\begin{aligned} \alpha &= \sqrt{28(1 + \frac{\eta^2}{3})} \\ \beta &= \frac{80(1-\eta^2)}{\alpha^3} \end{aligned} \tag{2.61}$$

The corresponding expression of the spin precision frequencies are

$$\begin{aligned} \omega_1 &= 2\sqrt{3}\alpha\omega_Q \sin(\frac{1}{3}arc\cos\beta) \\ \omega_2 &= 2\sqrt{3}\alpha\omega_Q \sin(\frac{1}{3}(\pi - arc\cos\beta)) \\ \omega_3 &= \omega_1 + \omega_2 = 2\sqrt{3}\alpha\omega_Q \sin(\frac{1}{3}(\pi + arc\cos\beta)) \end{aligned} \tag{2.62}$$

The value of the asymmetric parameter defined by equation (2.44), in the principal axes system with the convention $|V_{zz}| \leq |V_{yy}| \leq |V_{xx}|$, is restricted to $0 \leq \eta \leq 1$. Therefore, the electric field gradient tensor can be described for most applications by two parameters i.e; V_{zz} and η. The strength of the quadrupole interaction may

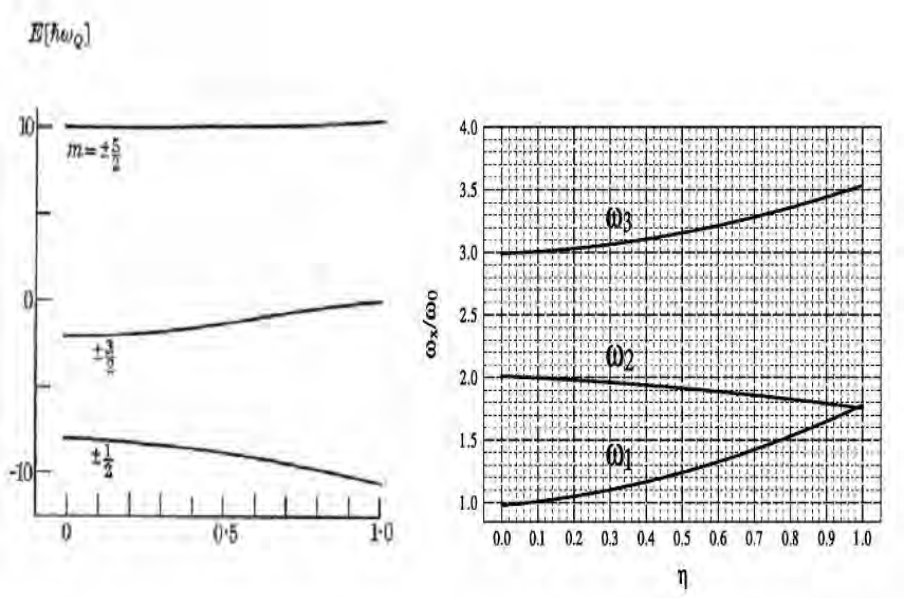

Figure 2.3: The splitting of the intermediate energy levels of spin I = 5/2 and associated transition frequencies as a function of the asymmetry parameter η according to eq. 2.61 and 2.63

be expressed by the interaction frequency (ν_Q):

$$\nu_Q = g(\eta)\frac{eQV_{zz}}{h} = g(\eta)\frac{10}{3\pi}\omega_1 \tag{2.63}$$

which is independent of the intermediate level spin. If $\eta = 0$, then $g = 1$. In the above theoretical considerations, the gradients are arising from charge distributions at lower cubic symmetry that surround the decaying nuclei are mainly responsible for the quadrupole interactions.

Chapter 3

The Perturbed Angular Correlation spectroscopy

3.1 Introduction

Perturbed angular correlation (PAC) spectroscopy is a nuclear technique based on nuclear interaction between electromagnetic moments of the nucleus (magnetic dipole moment and electric quadrupole moment) and extranuclear fields. These electromagnetic fields exert a torque on the moments which results in a precession of the moments.Measurements of hyperfine interaction in solids directly give the quadrupole coupling constant of the nucleus, and can be determine the symmetry of the field tensors.

The PAC technique requires the introduction of radioisotope probe atom that decay through $\gamma - \gamma$ cascades in the material host of interest. The directional correlation of the two emitted $\gamma-$ rays provides information on the electric or magnetic fields of the local environment of the probe. Quantum mechanically the perturbed angular correlation method consists basically on obtaining an ensemble of aligned nuclei in an excited state and measuring the angular distribution of the radiation emitted from this state. Alignment of an ensemble of nuclei is obtained when the

population of different magnetic sub-states are not equal but states with symmetric magnetic quantum numbers, $\pm m$, are equally populated. The work presented in this thesis involves only non-magnetic solids involving electric quadrupole interactions. According to the time behavior of the fields at the site of the nucleus, the interaction of the nuclear moment with the field can be static, periodic and time depend interaction but in this work, the static extranuclear interaction is considered. Therefore, the subsequent discussion will be restricted to electric quadrupole interactions in crystalline materials.

3.2 The Perturbed Angular Correlation

The perturbed angular correlation method consists basically in obtaining an ensemble of aligned nuclei in an excited state and measuring the angular distribution of the radiation emitted from this state. Alignment of an ensemble of nuclei is obtained when the population of different magnetic sub-states are not equal but states with symmetric magnetic quantum numbers, $\pm m$, are equally populated.

When the nucleus decays by the successive emission of two γ-rays in a cascade as shown in Fig.3.1, detecting γ_1 in a fixed direction selects an aligned ensemble of nuclei and the radiation γ_2 shows an angular correlation relative to the first direction.

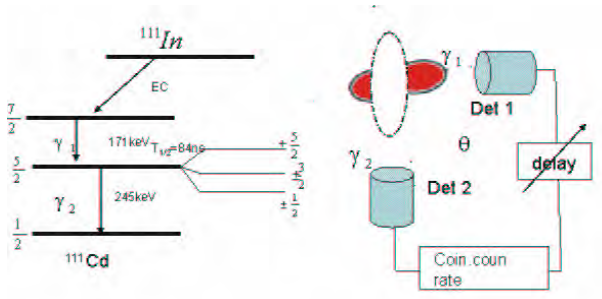

Figure 3.1: Decay cascade of an exited nucleus

The first ray γ_1 is associated with the transition from the initial nuclear state

$I_i M_i$ to the intermediate state IM which then decays to the final state $I_f M_f$ following the emission of the second gamma ray γ_2. If the populating γ_1 is detected in a certain direction by detector 1, a group of nuclei with particular spin orientation of the intermediate is selected. Due to angular momentum conservation, the distribution pattern of the depopulating γ_2 is spatially anisotropic. Since the anisotropic radiation pattern can only be observed with respect to the first populating gamma ray, the spatial distribution of the second gamma quantum is called an angular correlation.

An external electromagnetic field (i.e. EFG) at the site of the decaying nucleus will interact with electric quadrupole of the probe nucleus. These hyperfine interaction lift the degeneracy of the intermediate states. The amount of energy splitting is related to the strength of the local field. The intermediate state I is present only during the time between its formation and successive decay. This results in a time dependent angular distribution of the emitted radiation. This is characterized by the perturbation function G_{kk} which is related to the amount of energy splitting. If $\Delta E = E_m - E_{m'}$ is the energy difference between the two substates m and m', G_{kk} [3] has the form

$$\begin{aligned} G_{kk} &\sim exp[\frac{-it}{\hbar}\Delta E] \\ &\sim exp[-i\omega t] \end{aligned} \tag{3.1}$$

In a polycrystalline sample the electromagnetic fields at the site of the probe atoms have random orientation. In this case the angular correlation [3,5,23] is given by

$$W(\theta, t) = \sum_{k=0}^{K_{max}} A_{kk} G_{kk}(t) P_k(\cos\theta) \tag{3.2}$$

The value of K are in the range of $0 \leq K \leq$ minimum of $(2I, L_1 + L_1', L_2 + L_2')$ Where θ is the angle between the successive direction of emission. A_{kk} is angular correlation coefficient (depends exclusively on the nuclear property), which describe the deviation of the coincidence probability from the isotropic case $W(\theta) = 1$

[15]. $P_k(cos\theta)$ is legender polynomials, and it describes the spatial angular distribution of the $\gamma - ray$.

Equation (3.1) suggests that the perturbation function G_{kk} will result in the time dependent oscillation of the angular correlation with the spin precession frequency ω. The hyperfine interaction between the nuclear electric quadrupole moment with an external electric field gradient with axial symmetry [1,3,5], can be describe by the perturbation function in (3.2):

$$G_{KK}(t) = \sum_{n=0}^{3} S_{kn} \cos(n\omega_0 t) \tag{3.3}$$

Where ω_0 is the smallest precession frequency which can be observed (see equation 2.59) and n is a positive integer (including 0) with values $|m^2 - m'^2|$ and $\frac{1}{2}|m^2 - m'^2|$ for integer and half-integer I respectively. The coefficients S_{kn}, which correspond to the transition probabilities between sublevels are defined by.

$$S_{kn} = \sum_{m,m'} \begin{pmatrix} I & I & k \\ m' & -m & -m+m' \end{pmatrix}^2 \tag{3.4}$$

Numerical values for S_{kn} are tabulated for several values of the intermediate spin I in [15], for $k = 2$ and $I = 5/2$ the S_{2n} coefficients are $s_{20} = 0.2000, s_{21} = 0.3714, s_{22} = 0.2857, s_{23} = 0.1429$[7, 14].

For a non-axial electric field gradient, The perturbation function can still be written as in equation (3.3) but the S_{kn} coefficients and transition frequencies depend on the value of η:

$$G_{KK} = \sum_{n=0}^{3} S_{kn}(\eta) \cos(n_n(\eta)\omega_0 t) \tag{3.5}$$

In case of single crystal source Eq (3.2) is now no longer applicable because the angles, which the detectors 1 and 2 form with the direction of the V_{zz} component, have to be taken into account, and the angular correlation function has to be calculated separately for each detector arrangement. On the other hand, using

single crystals, the orientation of the field gradient tensor with regard to the crystal lattice can be determined by the measured amplitudes s_{2n} [7,6]. The correlation function of axially symmetric field of the single crystalline source of spin $I = \frac{5}{2}$ is defined as

$$R(t) \simeq G_{22} = \sum_{n=0}^{3} S_n^{eff}(\theta_1, \phi_1, \theta_2, \phi_2) \cos(n\omega t) \tag{3.6}$$

Where $S_n^{eff}(\theta_1, \phi_1, \theta_2, \phi_2)$ coefficients are drived using the function $Y_k^N(\theta, \phi)$ and ratios of the anisotropic coefficients [15]. Hence $Y_k^N(\theta, \phi)$ of the correlation function determines the modulation pattern of the orientation of the EFG with respect to the detectors.

3.3 Determination of R(t) function

In this section we will discuss how the data are measured experimentally and compared with appropriate theoretical perturbation functions. In measuring the angular correlation between γ_1 and γ_2 as a function of time elapsed between the arrival of both photons at least two detectors are necessary. The simplest form of the experimental set up is a two detector system in which one is fixed and the other one is movable (see figure 3.1). By detecting both γ_1 and γ_2 in coincidence, information can be obtained on the orientations of the same nuclear spins I at the times of the emission of the two γ rays, from the measured change of the spin orientation ΔI during the time t, elapsed between the emission of both gamma rays for an ensemble of probe atoms, the spin precession frequency ω is deduced. From such arrangements eight coincidence spectra $N_{ij}(\theta, t)$ are possible like the arrangement of four fixed detectors that each form 90 degree to each other. The coincidence count rate between two detectors i and j, whose axis form an angle θ with a radioactive at the vertex is given by [14].

$$N_{ij}(\theta, t) = N_0 exp(\frac{-t}{\tau_N}) W(\theta, t) + B_{ij}(\theta, t) \tag{3.7}$$

where t is the time interval between the detection of γ_1 and γ_2, N_0 is the number of cascades per unit time occurring in the sample, τ_N is the lifetime of the intermediate state, $W(\theta, t)$ is the correlation function of the γ cascade and $B_{ij}(\theta, t)$ is the background coincidences count rate. The first step in the evaluation of the experimental data is the subtraction of the background coincidences count rate. From the measured coincidence counting rates the ratio function R(t) was obtained by the following relation.

$$R(t) = 2[\frac{N(180^0, t) - N(90^0, t)}{N(180^0, t) + 2N(90^0, t)}] \tag{3.8}$$

$$R(t) = \frac{2}{3}[\sqrt{\frac{N_{13}(180^0, t)N_{24}(180^0, t)}{N_{14}(90^0, t)N_{23}(90^0, t)}} - 1] \tag{3.9}$$

But

$$\frac{2}{3}[\sqrt{\frac{N_{13}(180^0, t)N_{24}(180^0, t)}{N_{14}(90^0, t)N_{23}(90^0, t)}} - 1] \simeq A_{22}G_{22} \tag{3.10}$$

Hence $R(t) \simeq A_{22}G_{22}$. From the theoretical considerations, the perturbation function of axially symmetric field of the single crystalline source of spin $I = \frac{5}{2}$ is fitted with the experimental R(t)[7]

$$R(t) \simeq A_{22}G_{22}(t) = A_{22}\sum_{n=0}^{3} S_n^{eff}(\theta_1, \phi_1, \theta_2, \phi_2)\cos(n\omega_o t) \tag{3.11}$$

once we know the relation between the experimental measurable quantity R(t) and the perturbation factor $G(\theta_1, \phi_1, \theta_2, \phi_2, t)$. It is possible to determine ν_Q and η from the measurable spectra. R(t) is proportional to the perturbation function $G_{22}(t)$ which contains all the information regarding the hyperfine interaction between the nuclear moment and the crystalline field gradient.

Chapter 4

Result and Discussion

4.1 Introduction

Crystalline solids with atoms, ions or molecules of which they are composed falling into regular, repeated three dimensional patterns. Defects such as missing atoms, misplaced atoms and the presence of impurities have a considerable play role the physical properties of a crystal[16]. In semiconductor, it is common to find impurities, which are doped intentionally or undesirably during material processing. So, such situations can change the electrical and optical properties of the material by creating impurity energy level in the forbidden energy gap of the host material.

In the current presentation, silicon material is used which has diamond structure. In crystalline silicon, each atom makes covalent bond with the surrounding nearest atoms to form cubic environment. When we incorporate atoms, such as p, As, and Sb, which are donors in silicon, one extra electron will be in the vicinity and forms an energy level inside the forbidden gap. Similarly if we incorporate group three atoms such as B, Al, and In, their presence leaves vacancies called holes in the electron structure of the crystal lattice. Besides the existence of extra charges (i.e. electrons and holes), the entire charge distribution will be disturbed near the sites of impurity due to the size difference and change of different lattice parameters near the impurity. The formation of complexes of group three and five in silicon

semiconductor is by columbic attraction of oppositely charged atoms. The formation and the effects of group V (P, As) impurities on the behavior of indium atoms implanted into silicon single crystals was studied by Rutherford back scattering or ion channelling spectrometry, perturbed $\gamma - \gamma$ angular correlation, Infrared spectroscopy and resistivity measurements for high dos indium ion implantation on the past $[6, 7, 8]$.

Using perturbed $\gamma - \gamma$ angular correlation, we can measure the fraction of the total numbers of probe atoms in a particular environment. One can, therefore, determine the fraction of indium atom involved in Cd-impurity complexes, which is proportional to the impurities and a Boltzmann factor involving the complex's binding energy. It follows that, in a given material, at a given temperature, the measured fraction of indium -impurity pairs is directly proportional to the concentration of impurity. In the present discussion, results of the perturbed $\gamma - \gamma$ angular correlation (PAC), which is sensitive to the nearest neighbor defects. The population measurements of In-P pair in silicon at various annealing temperature will be presented.

4.2 Formation of In-p pairs in Silicon.

The samples were prepared from a Czochralski (CZ) grown silicon wafer with $< 110 >$ surface and the implantation were carried out in two steps, first the indium atom was implanted in a specified profile and then secondly the phosphorous impurity would implant on the same profile with that of indium. now, we are in a position to deal on the formation of In-P pairs in silicon crystal. we made the implantations using the ion implantation method. The impurity atoms, which are Indium and phosphorous were implanted or incorporated in the crystal silicon. Since the concentration of the dopants have an influence on the formation of pairs $In-P$, for the present work the impurities implantation dose were of $4 \times 10^{14} atoms/cm^2$ at $60kev$ and $8 \times 10^{12} atoms/cm^2$ at $160kev$ for P and In respectively. The implantation has held at the university of Bonn in mass separator facility. After the implantation of each impurities, there were formation of defects near the probe atom and these may create defects due to the high energy implantation. Such radiations damage would be recovered by annealing the samples at different temperature using the isochronal annealing program. In case of this work, the radiation damage was recovered at annealing temperature of $627^o c$ with well defined interaction frequency of the In-P pair [7]. All the measurements were performed by the perturbed angular correlation technique, which is clearly discussed in the previous chapter of this thesis. In the current work, one can able to see the formation of In-P pairs at different annealing temperature as well as the variation of the population and other important parameters of the Hyperfine interaction.

4.3 Result and discussion

After the post-implantation of phosphorous, a typical R(t) spectrum is shown in Fig 4.1, for the annealing temperature of 700^oc, 900^oc, 700^oc, 1000^oc and 700^oc at annealing rate of 10, 10, 30, 10 and 40 minutes respectively.

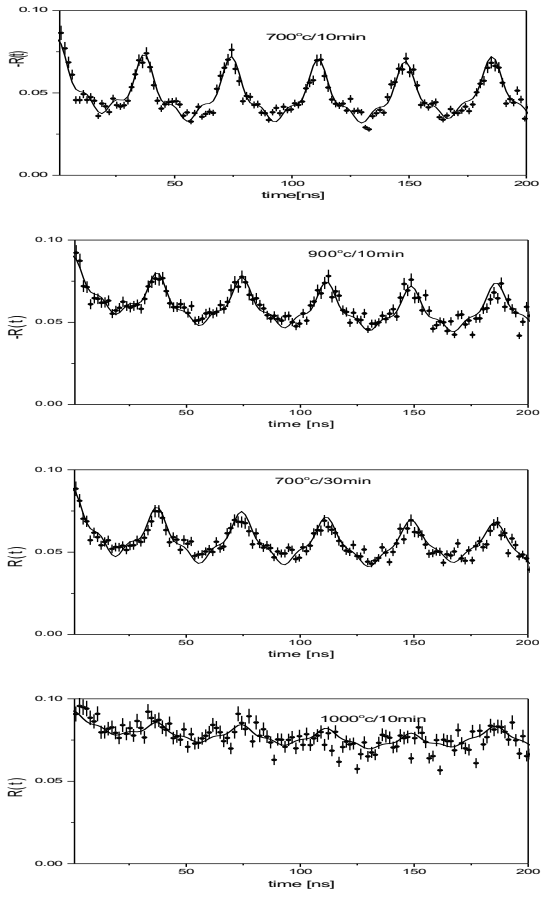

Figure 4.1: PAC time spectra modulated by the interaction frequency of In-P pair in silicon.Measurement are taken along $< 110 >$

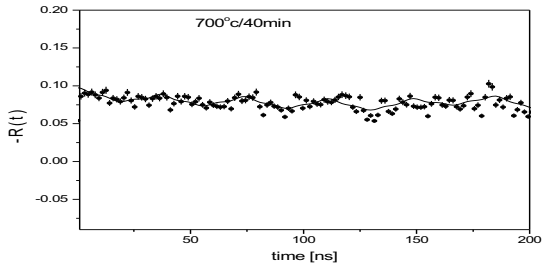

Figure 4.2: PAC time spectra modulated by the interaction frequency of In-P pair in silicon.Measurement are taken along $< 110 >$

The measurements observe the interaction at the intermediate state $I = \frac{5}{2}$ and the population of the pair ^{111}Cd-p has been influenced by the annealing temperature T_a. The Cd-P implantation at room temperature causes radiation damage and starts amorphization of the Si crystal. During annealing up to 700^oC, recrystallization occurred and the formation of Cd-P complex was formed with the observation of the well defined quadrupole interaction frequency [7, 13]. When the sample is annealed at temperature of 700^oC for 10 min, the fractional population of the complex would be $27(2)\%$. For the annealing temperature $T_a > 700^oC$, the ^{111}Cd-P complex starts to dissociation because the thermal energy attained by the complex at high temperatures exceeds the binding energy that keeps them together. Hence, After annealing the sample at 900^oC for 10 min, the fractional population dropped to $16(1)\%$. whereas, the fractional population of the tetrahedrally symmetric substitutional site of indium grows to nearly to $66(1)\%$ at 900^oC. The sample was then annealed again at 700^oC for 30 minutes, and the PAC data showed an increase in the pair fractional population to $21(1)\%$. This change can be seen in Fig 4.1 by the amplitude change of the modulation in the PAC time spectra. The results are summerized in table 4.1.

T_a	In-P substitutional	Cubic	undefined
$700^oC/10$ min	27(2)	57(1)	16
$900^oC/10$ min	16(1)	66(1)	18(1)
$700^oC/30$ min	21(1)	60(1)	19(1)
$1000^oC/10$ min	5(2)	76(2)	19(2)
$700^oC/40$ min	7(1)	73(1)	18(1)

Table 4.1: Fit results of In-P pair in Si

All the Panels of fig 4.1 and 4.2 shows the PAC signal modulated by a well defined interaction frequency of $\nu_Q = 179(1)$ MHz and this result is in agreement with previous report $[7, 8]$. The observed frequency modulation resulted from the formation of a unique probe defect complex in the sample is assigned to the formation of the substitutional $^{111}Cd - P$ pair in the silicon. Since, this frequency has never been observed in any intrinsic silicon or even there is no report of the frequency of this nature in Other impurity doped silicon at these T_a.

The orientation measurement also characterizes the pair ^{111}Cd-P and we measured by directing the major crystal axis toward the detectors, (i.e. $< 100 >, < 110 >, < 111 >$). This measurement suggests that orientation of the major component of EFG tensor (V_{zz}) lies along $< 111 >$ [20], but it's symmetry is determined from the value we observed in the fit result, (i.e. $(\eta = 0)$). In this measurement, we observed only one frequency for the values of the T_a shown in fig 4.1 and then the frequency eventually disappears above 1000^oC [7]. More phosphorous clusters could be observed when phosphorous is doped at the time of crystal growth $[6, 7, 8]$. So, the results we observed here is only one, since phosphorous was incorporated using the implantation method. The two possible sites are

Site 0 stands for an indium surrounded by four identical host atoms and form cubic environment. In this site the indium can not experience an EFG, as the charge distribution at the Indium probe is symmetric in diamond lattice. The second site with one impurity atom next to the probe atom and this breaks the symmetry of the charge distribution , which leads to a unique EFG.

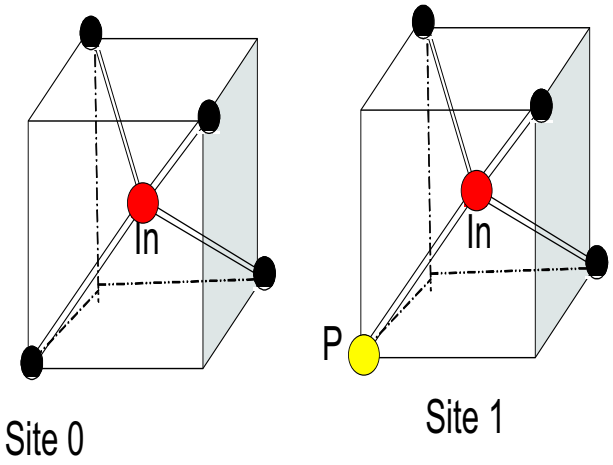

Figure 4.3: Models representing possible substitutional indium environment in Si, where the black balls are host atoms

The anisotropy coefficient of as $A_{22} = -0.1050$, this is the effective spatial anisotropy of the $\gamma - \gamma$ angular correlation. This result is some what deviated from theoretical values given in [3]. The frequency of modulation of the R(t) signals is proportional to the strength of the electric field gradient at the probe nuclei (^{111}In), which is clearly discussed in chapter two of this thesis. The EFG can be calculated through

$$\nu_Q = \frac{eQV_{zz}}{h} \tag{4.1}$$

The measured frequency corresponds to the EFG (i.e. $8.9 \times 10^{17} \frac{V}{cm^2}$) is the result of an asymmetric charge distributions caused by either the presence of near by defects and/or unpaired localized charge at the site of the probe atom. In general, the magnitude of the EFGs vary with the type of impurities [7, 8, 13]. The measured EFG also affected by the size of the impurity incorporated in and lattice location of an impurity, since the EFG depends on r^{-3}[7,8,9].

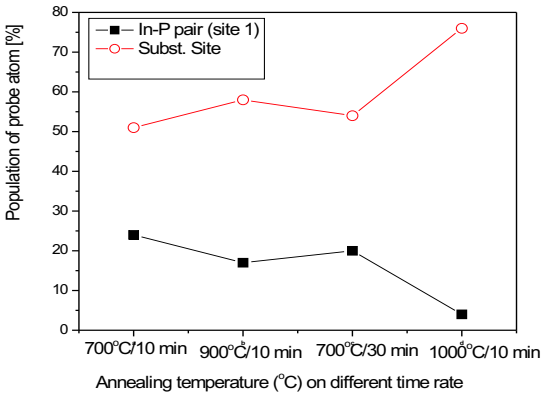

Figure 4.4: The fractional population of indium at different environment in different annealing temperature with different rate.

4.4 Dependence of the defect fraction on annealing temperature.

Temperature dependence of the fractional population f of In-P pair in silicon was studied for annealing temperatures above 700^oC. A decrease in f with higher annealing temperatures is shown by decrease in the oscillation amplitude in R(t) spectra (see figure 4.1).

In the following sections based on the thermodynamics of the equilibrium concentration of acceptor-donor pairs and the binding energy of the site 1 was calculated using the fraction of the pairs obtained from the PAC experiment in table 4.1.

4.4.1 Determination of the binding energy for Impurity pairs

The fraction of the probe atom forming the complex ^{111}Cd-P was determined at each annealing temperature see table 4.1. The impurities were incorporated to the silicon crystal with dose of $4 \times 10^{14} atoms/cm^2$ and $8 \times 10^{12} atoms/cm^2$ for phosphorous and Indium impurity respectively. Using the concept of free energy, one can describe the ratio of number of impurity pair in silicon to their constitues or free

state. The free energy F of the whole crystal after incorporating the impurities is given by [14,17].

$$\begin{aligned} \frac{n_{In-P}}{N} &= \frac{(n_P - n_{In-P})(n_{In} - n_{In-P})}{N^2} Z exp[\frac{S_{In-P} - S_P - S_{In}}{K}] \\ &\times exp[\frac{-(E_{In-P} - E_P - E_{In})}{KT}] \end{aligned} \tag{4.2}$$

Where $E_{In-P} - E_P - E_{In} = \varepsilon$ is the negative of the binding energy which is equal to the energy difference between the trapped and free state. N is the number of lattice sites of the sample in which the impurities as well as the pairs can be arranged on. n_P, n_{In} and n_{In-P} are the number of isolated atoms P, In and In-P. $S_{In-P} - S_P - S_{In} = \Delta S$, which is the difference in vibrational entropies for the pair and for isolated impurity sites. Z is the coordination number of the lattice (for tetrahedral lattice, $Z = 4$). If the vibrational entropy effects is neglected and N>> n_P, n_{In}. Equation (4.2) can be written as

$$C_{In-P} = C_P C_{In} B exp[\frac{-\varepsilon}{KT}] \tag{4.3}$$

Where C represents concentration. Commonly, the binding energy E is defined as positive (i.e. E=-ε). Measurements of the temperature dependence yield the information on the binding energy. The slope of the Arrhenius plot $\ln(\frac{C_{In-P}}{C_{In}C_p})$ Vs $\frac{1}{T}$ gives the binding energy. Equation 4.3 can be written as

$$\ln(\frac{C_{In-P}}{C_{In}C_p}) = \ln(B) + \frac{E}{KT} \tag{4.4}$$

Where E is the binding energy and B is the ratio of free and trapped state around the complex formed. Therefore, using the fractional population of the pairs obtained from PAC data with the annealing temperature interval of $700^oC - 1000^oC$, one can be able to calculate the binding energy of the pair in site 1 (see figure 4.3). The observed ratio $\frac{f}{1-f}$ is equal to $\frac{C_{In-P}}{C_{In}}$, i.e., to the ratio of the Indium atoms bound with one phosphorous impurity to the concentration of Indium atoms surrounded by the host atoms only. Knowing the nominal phosphorous concentration C_p the

Annealing temperature (T_a)[K]	reciprocal of $T_a[K^{-1}]$	$\frac{C_{In-P}}{C_{In}}$
973	0.00103	0.37
1173	0.00086	0.19
1273	0.00078	0.05

Table 4.2: The ratio of fractions of the pair to fraction of the impurity

$\frac{C_{In-P}}{C_{In}C_p}$ was determined. This is taken under the condition that the equilibrium state is reached at each annealing temperature. The ratio of fractions paired to fraction of the probe atom obtained from fit of PAC data given in table 4.1 is tabulated in table 4.2.

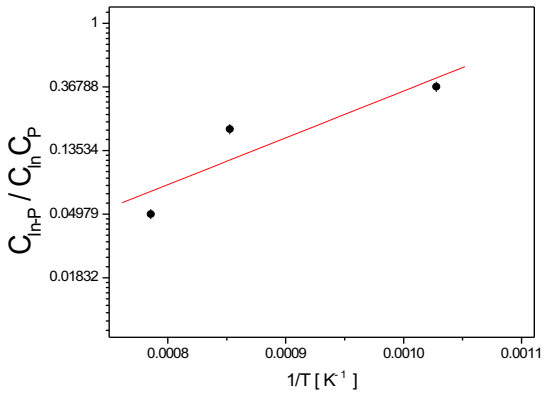

Figure 4.5: Relative fraction of In-P complexes in silicon as a function of the inverse temperature. The straight line is a fit of (4.4) to the experimental data.

Figure 4.4 show Values of $\frac{C_{In-P}}{C_{In}C_p}$ plotted on a logarithmic scale verses $\frac{1}{T}$. The straight line in Fig. 4.4 is least squares fit of Equation 4.4 to the experimental data with B and E being free parameters. Therefore, the slope of the plot in fig 4.4 gives the binding energy E of the In-P pair, that is 0.64eV and. The result deviates from the value obtained using coulombic attraction between a single donor and an acceptor as nearest neighbors in silicon $(0.5eV)$. In literatures [7], the binding energy of the different group five donors with Indium atom was reported (see table

pair	In-P	In-As	In-Sb
ν_Q(MHz)	179(1)	229(1)	271(1)
E_B(eV)	0.69	0.54	0.32

Table 4.3: Binding energy of the indium donor pair in Si [7]

4.3). The value obtained in this work is near to the result reported for In-P pair in previous report. The binding energy calculated in this thesis is based on the fractional population obtained from the PAC data, as given in table 4.1 and 4.2.

From table 4.3, one can see group five atoms bound with Indium atom. The values show that the strength of the chemical bonds they have. From this point of view, one can observe that the binding energy decreases with increasing atomic size. We can also conclude that the re trapping of donors after dissociation of the pairs could successfully be observed for the donors having less binding energy.

From the results discussed so far, the binding energy of the pair formed in site 1 is 0.64eV, this result is nearly similar to the previous report in Table 4.3 [7]. The second free parameter in equation 4.4 is also found from the fit of the experimental data (i.e., B) and its value is 7×10^2. As B represents the ratio of free and trapped states around ^{111}Cd-P complex.

In this thesis, the proposed structural model, the measured electric field gradient using the PAC method have shown a remarkable agreement with theoretical calculations as well as with others previous reports [7,13]. The measured binding energy using the PAC method also have shown a remarkable agreement with the previous report [7]. Specifically, knowing the number of fractions in the sample can help us to understand the effects of the pairs on electrical or optical properties of materials [6]; that's why this technique is applicable for material science. So, from this nuclear technique, one can be able to study the properties of semiconductors by investigating the microscopic environments of the atoms such as crystal field gradient,(i.e. EFG).

The study of problem dealing on the variations of the population of the ^{111}Cd-P complex with annealing temperature enable us to determine the binding energy of

the complex and the ratio of free and trapped states.

Conclusion

In this work, the formation of ^{111}Cd-P complex was studied using the perturbed angular correlation spectroscopy. By fitting the experimental data with the theoretical perturbation functions, we have determined the interaction parameters. From the time spectra taken at various annealing temperatures showed unique quadrupole interaction frequency associated with the presence of phosphorous in silicon. All the spectra shows an interaction frequency of $\nu_Q = 179$ MHz, which is associated to the complex. This frequency represents the formation of ^{111}Cd-P in silicon. The measurements suggest that the orientation of the major component of EFG tensor (V_{zz}) lies along $< 111 >$. The frequency damping $\delta = 0.86\%$ is determined for spectrum taken at $700^oC/30$ minutes and $\delta = 0.29\%$ for all other spectra.

The variation of the population of the ^{111}Cd-P complex with annealing temperature was observed. Therefore, from the fraction of probe atom at site 1, we have determined the binding energy of the complex by taking the temperature interval $700^oC - 1000^oC$. The value of the binding energy and the ratio of free and trapped states are obtained as 0.64eV and 7×10^2 respectively.

Appendix A

A The Wigner Eckert theorem

Matrix elements $\langle jm|T_q^k|j'm'\rangle$ separates in to two parts, one of them containing information on the magnetic quantum numbers, and the other part containing more the characteristics of the eigen vectors and operator. The Wigner-Eckart theorem separates this dependence in a specific way by the result.

$$\left\langle jm|T_q^k|j'm'\right\rangle = (-1)^{j-m} \begin{pmatrix} j & k & j' \\ -m & q & m' \end{pmatrix} \langle j||T^k||j'\rangle$$

The double-barred matrix element is the reduced matrix element. Its value does not depend on the z components m', m, and q. Whereas the angular momentum dependence expresses through the Wigner 3j-symbol.

B The 3-j symbols

Calculation of the $3-j$symbols for $k=2$ and spin $I=\frac{5}{2}$ For any angular momentum $j_1, j_2, j_3$with projection m_1, m_2, m_3 respectively is given by relation.

$$\begin{pmatrix} j_1 & j_2 & j_3 \\ m_1 & m_2 & m_3 \end{pmatrix} = (-1)^{j_1-j_2-m_3} \triangle(j_1, j_2, j_3) W_3(j_1, j_2, j_3, m_1, m_2, m_3)$$

where

$$\triangle(j_1, j_2, j_3) = [\frac{(j_1+j_2-j_3)!(j_1-j_2+j_3)!(-j_1+j_2+j_3)!}{(j_1+j_2+j_3+1)!}]^{\frac{1}{2}}$$

$$\begin{aligned} W_3(j_1, j_2, j_3, m_1, m_2, m_3) &= [(j_1+m_1)!(j_1-m_1)!(j_2+m_2)!(j_2-m_2)!(j_3+m_3)!(j_3-m_3)]^{\frac{1}{2}} \\ &\times \sum_{\nu} \frac{(-1)^{\nu}}{\nu!(j_1+j_2-j_3-\nu)!(j_1-m_1-\nu)!(j_2-m_2-\nu)!} \\ &\times \frac{1}{(j_3-j_2+m_1+\nu)!(j_3-j_1-m_2+\nu)!} \end{aligned}$$

Where the summation is over zero and positive values of ν for which the factorial is not negative. Using this formula we can evaluate the $3-j$ symbols as where$j_1 = j_3 = I$, $j_2 = 2$,$m_1 = -m$, $m_2 = 0$ and $m_3 = m$ follows

$$\begin{aligned} \begin{pmatrix} I & 2 & I \\ -m & 0 & m \end{pmatrix} &= \sqrt{\frac{(2)!(I-2+I)!(2)!}{(I+2I+1)!}} [(I+m)!(2)!(2)!(I-m)!(I+m)!]^{\frac{1}{2}} \\ &\times \sum_{\nu} \frac{(-1)^{\nu}}{\nu!(2+I-I-\nu)!(I+m-\nu)!(2-0-\nu)!} \\ &\times \frac{1}{(I-2-m+\nu)!(I-I-0+\nu)!} \end{aligned}$$

Where $\nu = 0, 1, 2$ (since the other terms make the factorial negative).Therefore we can write the matrix as follows

$$\begin{pmatrix} I & 2 & I \\ -m & 0 & m \end{pmatrix} = \frac{2(3m^2 - I(I+1))}{[(2I+3)(2I+2)(2I+1)(2I)(2I-1)]^{\frac{1}{2}}}$$

The same is true for the following matrix

$$\begin{pmatrix} I & 2 & I \\ -I & 0 & I \end{pmatrix} = \frac{2I(2I-1))}{[(2I+3)(2I+2)(2I+1)(2I)(2I-1)]^{\frac{1}{2}}}$$

The quotient of the two matrix is

$$\begin{aligned} \frac{\begin{pmatrix} I & 2 & I \\ -m & 0 & m \end{pmatrix}}{\begin{pmatrix} I & 2 & I \\ -I & 0 & I \end{pmatrix}} &= [\frac{2(3m^2 - I(I+1))}{[(2I+3)(2I+2)(2I+1)(2I)(2I-1)]^{\frac{1}{2}}}] \\ &\div [\frac{2I(2I-1)}{[(2I+3)(2I+2)(2I+1)(2I)(2I-1)]^{\frac{1}{2}}}] \end{aligned}$$

Therefore

$$\frac{\begin{pmatrix} I & 2 & I \\ -m & 0 & m \end{pmatrix}}{\begin{pmatrix} I & 2 & I \\ -I & 0 & I \end{pmatrix}} = \frac{3m^2 - I(I+1)}{I(2I-1)}$$

Bibliography

[1] Schatz.G and Weiding.A (1996), ”Nuclear condensed matter physics”, chapter 2, 3, 4. Wily, Newyork.

[2] G.Tessema and R.Viander, ”Indium-carbon pairs in germanium”; J.phys; condens. matter **15** (2003), pp5297-5306

[3] Th.Wichert and E.recknagel, ”Perturbed Angular Correlation”

[4] David Blecker and George CsoBasic partial Differential Equationby Nostrand and Reinhold, New York pp.612 (1992)

[5] R.M.Steffen and K.Alder, ”The Elctromagnetic Interaction In Nuclear Spectroscopy”, North-Holland, 1975.

[6] S. Yu. Shiryaev and A. Nylandsted Larsen, ”The chemical interaction between high-concentration, mixed ion implanted group-III and -V impurities in silicon”, Journal of Applied Physics, Volume **72** (1992), Issue 2, pp. 410-421

[7] G.Tessema, ”Indium-impurity pairs in semiconductors and the study of the influence of uniaxial stress on defect complexes in silicon”, PhD. disertation, (2003), Bonn University, Germany.

[8] M. L. Swanson, Th. Wichert, and A. F. Quenneville, ”Detection of In-P and In-Sb atom pairs by perturbed angular correlation in silicon” Applied Physics Letters, Volume **49** (1986), Issue 5, pp. 265-267

[9] Teshome senbeta, "Temperature dependent of Hyperfine Interaction in ^{111}Cd Nuclues", Msc. Thesis, Addis Ababa University, (2005)A.A.

[10] Richard N.Zare, Angula rmomentum understanding spetial aspects in chemistry and physics, John Wiley and Sons, Inc. pp 49-51 (1988).

[11] Philipp Gütlich, Rainer link, Alfred Trautwein, "Inorganic Chemistry concepts" **3**, Springer-Verlage, Berline Heidelberg, New York.

[12] DONALD A. NEAMEN, "Semiconductor Physics and Devices", Basic Principles, (1992).

[13] A. Burchard, M.Deicher, Th.Wichert, "Electric Field Gradients of Acceptor-Donor Pairs in semiconductor", CH-1211 Geneva 23, Switzerland.

[14] Paulo Jorge Baeta Mendes, "H-O (H-N) complexes in metals, studied by perturbed angular correlations" PhD. disertation University of Coimbra(1987).

[15] H. Frauenfelder, R. M. Steffen; Alpha-, Beta- and Gamma Spectroscopy, Vol. 2, Ed., K. Siegbahn pp. 997 (1965).

[16] A. Beiser, Concepts of Modern Physics, Mc Graw Hill, Inc. Fifth Ed. New York, PP. 354-357 (1995).

[17] A.Z.Hrynkiewicz and K. Krolas; Formation of two-impurity complex in dilute alloys observed through perturbed angular correlation of $\gamma-$ rays; Phys. Rev. B Vol. 28 No. 4 pp. 1864-1869(1983).

[18] Elton N.Kaufmann and Reiner J. Vianden, "Electric field gradient in non cubic metals" Rev.Mod.phys Vol **51**, No.1, pp.173 (1979).

[19] N.Thomas Olson, Experiments in Modern Physics, McGraw Hill, Inc. New York, PP. 160 (1966).

[20] M.L.Swanson. Th, Wichert and A.F.Quenneville; Detection of In-P and In-Sb atom pairs by PAC; App. Phy. Lett. Vol. 49 No. 5 pp. 265-267(1986).

[21] J.C.Austine, Wm, C.Hughes, B.K. Patnaik,, R.Triboulet; PAC studies of In-Vacancy pairs in $Hg_{1-x}Cd_x$Te; Jour. App. Phy. VOl **86**, No.7, pp.3577 (1999).

[22] Kurt Alder, Eckat Matthias, Werner Schinder, Rolf M.Steffen; Influence of a cobined magnetic dipole and electric quadrupole interaction angular correlations, Phys. Rev. Vol.129 No.3 pp. 1199-1213(1962)

[23] E.Gerdau; J.Wolf; H.Winkler; J.Braunsfurth, "Quadrupole Interaction of 181 Ta in Hf Compounds", Royal Society of london, series A, pp. 197-206. Jun. 24, (1969).

DECLARATION

I the under signed declare that the thesis is my original work, has not been presented for a degree in any other university and that all sources of material used for the thesis have been duly acknowledged.

Temesgen Yirdaw

Signature: _____

This Thesis has been submitted for examination with my approval as university advisor.

Dr. Genene Tessema

Signature: _____